Published in final edited form as:
Coord Chem Rev. 2008 February ; 252(3-4): 347–360. doi:10.1016/j.ccr.2007.08.022.

Photoassembly of the Water-Oxidizing Complex in Photosystem II

Jyotishman Dasgupta[†], **Gennady M Ananyev**[‡], and **G. Charles Dismukes**[*,‡]

† *306 Lewis Hall, Department of Chemistry, University of California, Berkeley, CA 94709, USA*

**7 Hoyt Laboratory, Department of Chemistry, Princeton University, Princeton NJ 08544, USA*

Abstract

The light-driven steps in the biogenesis and repair of the inorganic core comprising the O_2-evolving center of oxygenic photosynthesis (photosystem II water-oxidation complex, PSII-WOC) are reviewed. These steps, known collectively as photoactivation, involve the photoassembly of the free inorganic cofactors to the cofactor-depleted PSII-(apo-WOC) driven by light and produce the active O_2-evolving core comprised of $Mn_4CaO_xCl_y$. We focus on the functional role of the inorganic components as seen through the competition with non-native cofactors ("inorganic mutants") on water oxidation activity, the rate of the photoassembly reaction, and on structural insights gained from EPR spectroscopy of trapped intermediates formed in the initial steps of the assembly reaction. A chemical mechanism for the initial steps in photoactivation is given that is based on these data. Photoactivation experiments offer the powerful insights gained from replacement of the native cofactors, which together with the recent X-ray structural data for the resting holoenzyme provide a deeper understanding of the chemistry of water oxidation. We also review some new directions in research that photoactivation studies have inspired that look at the evolutionary history of this remarkable catalyst.

Keywords

Bicarbonate; Calcium; Manganese; photosynthesis; water oxidation; oxygen-evolution; Photosystem II

Introduction

The process of oxygenic photosynthesis is responsible for producing nearly all atmospheric O_2 on Earth by the light-driven oxidation of water[1]. However, oxidation of water to O_2 is a mechanistically complex and highly energy demanding chemical reaction [2]driven by photooxidation of a chlorophyll with electrochemical reduction potential of ca. 1.2-1.3 V [3]. In nature, this reaction proceeds by using the visible light energy that is trapped and made chemically available by chlorophyll photo-pigments, and it is ultimately carried out at the inorganic active site ($Mn_4O_xCa_1Cl_y$), the water-oxidizing complex (WOC), of a membrane

‡CORRESPONDING AUTHORS FOOTNOTE: G. Charles Dismukes, Department of Chemistry and Princeton Environmental Institute, Princeton University, Princeton, NJ 08544. Phone: 609-258-3949. Fax: 609-58-1980 dismukes@princeton.edu. Jyotishman Dasgupta dasgupta@berkeley.edu.

**PLEASE NOTE THE ORDER OF THE AUTHORS.

spanning protein complex known as photosystem II (PSII) [4]. Although nature has devised a very efficient way for oxidizing water, the coupling of the water-splitting reaction to the PSII reaction center photochemistry (chlorophyll photooxidation) takes a heavy toll on the protein matrix due to the generation of highly reactive chemical intermediates under illumination. The damage done to the D1 subunit requires its resynthesis and replacement within the 19-31 subunits of PSII, as well as the reassembly of the inorganic catalyst. This process can occur as frequently as every 30 min at full solar flux [5,6]. Reassembly of the inorganic cluster ($Mn_4Ca_1O_xCl_y$) of the water-oxidizing complex (PSII-WOC) is known as photoactivation; named by George Cheniae and coworkers the discoverer of this phenomenon (reviewed in [7]).

In this article we review the chemistry behind this complex photoassembly process focusing on the inorganic principles and the functional role of the cofactors in catalyzing the water oxidation chemistry. This chemistry is responsible for the concerted four-electron oxidation of two water molecules to make O_2 after injection of the fourth hole (electron vacancy) into the WOC. The thermodynamic efficiency of this chemistry has never been replicated in any abiotic catalyst of any kind. Unlike the reasonably well understood principles of single-electron and single-proton transfer chemistry, complex multi-electron/proton reactions control the overall energetics and thus the allowed pathway for catalysis [8,9,10]. Interested readers should also consult other recent reviews that cover *in vitro* and *in vivo* photoactivation of the WOC [11,12,13].

1.1 Photosystem II: A structural snapshot

The membrane-spanning PSII protein complex is assembled *in vivo* as a functional dimer with 19-31 subunits[14,15] in each monomer, depending on the organism in question. Only within the last three years, has the structural arrangement of each subunit, with respect to each other, been resolved by X-ray crystallography to 3–3.5 Å resolution with considerable certainty (R-factor = 24 %) [16,17]. PSII isolated from *Thermosynechococcus sp*. in its resting oxidation state has provided a more detailed structural model than was previously available from spectroscopic and mutagenesis studies alone. However, there has been noticeable differences in the two recent structures one at 3.0 Å [16] by Loll et al., and another at 3.5 Å by Ferriera et al. [17]. The structure of the active site of PSII along with the molecular modeling of the architecture near the water oxidation site from the 3.5 Å structure is shown in Fig 1. The modeling of the exact position of the metal ions inside the electron density representing the Mn_4Ca-cluster has been especially debated. The Imperial College group has postulated an assignment for all the elements in the WOC at 3.5 Å, while the Berlin group has left it as an open question by showing only the heavy atom scatterers [16,17]. A recent Mn EXAFS study of single crystals of these PSII core complexes has provided more evidence to distinguish between these models[18]. Also questions have arisen on the radiation damage to the cluster accrued by the X-rays used for the diffraction studies [19]. The Imperial College group has provided an alternative interpretation of the original electron density map that can be found in this special issue. However, the modeling of the protein subunits remains very similar from both groups. Importantly, it is now known how the extrinsic proteins are located with respect to the cluster. This information is valuable since it has been known that although an intact PSII core complex is needed for sustained O_2 evolution *in vivo*, some PSII subcore complexes lacking the extrinsic subunits can also produce O_2 *in vitro*. The smallest isolated reaction center (RC) complex that performs primary charge separation contains four subunits: D1 (*psbA* gene), D2 (*psbD* gene), and the two subunits of cytochrome *b*559, α (*psbE* gene) and β (*psbF* gene) along with another chloroplast encoded protein psbI [20,21]. These four subunits along with two membrane spanning chlorophyll binding proteins CP47 and CP43 comprise what is called the PS II core. No complex without these six subunits had been isolated that evolved oxygen [22]. However, a complex completely devoid of CP43 was shown to be photoactivatable (i.e.

showed O_2 activity when the cluster was reconstituted), albeit with much lower photochemical quantum yield and to a lower level of activity[23]. The D1 polypeptide provides most of the amino acid residues comprising the active site surrounding the cluster, with a notable contribution by residues Arg357 and Glu354 from CP43 in the active site. The structures coupled with the numerous mutational experiments and spectroscopic measurements have provided a lot of constraints to the mechanism of water oxidation which are briefly touched below. However, detailed discussion of possible mechanisms is beyond the scope of this review (for earlier reviews [24,25]).

1.2 Mechanistic questions on water oxidation

For the water oxidation reaction to take place, the cluster cycles through five oxidation states (named, in order, as S_i: i=0, 1,…, 4) starting from the resting state S_1, before it releases a dioxygen molecule and total of four substrate protons (through the S-state cycle). Stabilization of the higher oxidation states (S_2- and S_3-states) in the Mn_4Ca cluster is both due to the delocalization of positive charge among metal centers and also from a local electrostatic effect generated by the presence of strong sigma donor ligands such as aspartate, glutamate and histidine that surround the cluster in the active site. The role of the inorganic cofactors (Mn^{2+}, Ca^{2+}, Cl^{-}) in actual water oxidation chemistry has been subject to immense scrutiny. Numerous synthetically inspired and structure based proposals have been formulated. Proposals ranging from homolytic O-O bond formation from two facial bridging electron-deficient oxo's [25] to heterolytic O-O bond formation via nucleophilic-electrophilic oxo-coupling have been presented [26,27]. And although various spectroscopic and structural markers (such as EPR and EXAFS)[28,29,30], mutagenesis [31] and water exchange rates of the individual S-states have been considered [32], no commonly agreed on mechanism of water oxidation has been convincingly proved. It is for these reasons that the photoassembly reaction of the Mn_4Ca cluster provides special insights as it can dissect the roles of the individual cofactors and enables examination by substitution, a topic we refer to as "inorganic mutants".

1.3 PSII damage and repair

1.3.1. Protein Assembly—All the mechanisms of water oxidation proposed to date involve highly reactive oxidized manganese ions. However, under normal environmental conditions such as high light flux and ambient atmospheric O_2 pressure these intermediates can furnish radicals that are lethal and destroy the protein itself, leading to photoinhibition [33]. Loss of PSII activity by photoinhibition occurs as often as every 15-30 minutes under normal solar flux conditions. To cope with photoinhibition, oxygenic phototrophs have evolved repair and photo-protective mechanisms permitting a high rate of metabolic turnover of PSII polypeptides with the D1 protein exhibiting the highest rate of turnover. Since D1 appears to supply most of the protein-derived ligands to the Mn_4Ca, the frequency of *in vivo* photoactivation must follow the D1 protein repair rate. The site of the light reactions of oxygenic photosynthesis in cyanobacteria, green algae and plants (in the chloroplast) is a specialized inner membrane called the thylakoid membrane system. In higher plants, the initial dissociation of a damaged PSII dimer into monomers in the stacked grana regions of the thylakoid membrane system and further migration to the stromal region (outside the thylakoid membrane), starts the process of repair. However, it is not clear whether photoactivation of the inorganic cofactors of the WOC occurs within PS II complexes bound to the stacked grana membranes or within the stromal region. In the PSII repair process in cyanobacteria, evidence for the initially assembled RC with D1, D2 and cyt b559 subunits in the (non-photosynthetic) plasma membrane has been established, but not with CP43 or CP47 subunits [6]. Also, these partially assembled reaction centers in the plasma membrane can carry out charge separation and single turnover electron transfer [34]. The absence of CP47 and CP43 indicates that assembly of a functioning WOC is highly unlikely in the plasma membrane. Recent claims have been put forth by Chow and Aro that in the repair process CP47 is probably only partially disassembled. They also state

that CP43 is indisputably dissociated and re-attached along with PsbH and PsbL, both subunits are important in supporting CP43 re-assembly for repair in higher plants [33,35]. This evidence then gives credence to the proposal that Mn_4Ca could be photoassembled in the stromal region of the thylakoid membrane [33]. Observations on isolated PS II sub-complexes from which both CP43 and CP47 have been dissociated by detergents shows that these do not assemble a functional inorganic core during photoactivation, while the CP47RC sub-complex lacking only CP43 can be photoactivated, although the O_2 evolution rate is 20% that of photoactivated PSII membranes and highly unstable [23].

In the vast majority of organisms containing PSII, the D1 protein is synthesized as a precursor protein (pD1 with a short peptide extension (8–16 amino acid residues) on the carboxy terminus (C-terminus) that is proteolytically removed during the assembly process [12,36]. Experimental deletion of this segment still allows functional assembly of the WOC, provided the native mature C-terminal α-carboxylate at position 344 is available. The D1 C-terminal extension was shown not to be required for assembly of functional PS II complexes, nor for growth under optimal conditions in both *Synechocystis 6803* [37] and *Chlamydomonas* [38]. However, the carboxyl extension must be cleaved beyond Ala 344 by a soluble protease, called ctpA, prior to assembly of an active inorganic core [37,39]. This cleavage is essential for the assembly of the Mn_4Ca-core and, hence, oxygen evolution. Alanine 344, which is at the terminus of the mature D1, is proposed to ligate the Mn_4Ca through its backbone α-carboxyl moiety. While evidence is strong that the carboxyl group of D1–Alanine 344 is in close proximity to the Mn_4Ca, it is not resolved whether it ligates Mn or Ca. In the X-ray structure models based on crystals diffracting to 3.0 Å and 3.5 Å, the 3.0 Å structure places the C-terminus as coordinating Mn, whereas the 3.5 Å structure model orients the C-terminal carboxy moiety towards a calcium atom. Although the 3.0 Å structure shows possible Ca^{2+} ligation, authors use results from FTIR light-dark difference spectroscopy to argue against it [16]. They conclude that Ala344 is ligated to one of the Mn-atoms. Controversially however, in *Synechocystis* 6803 cultures which lack the carboxyl extension or have a genetically engineered two-fold longer extension exhibit no difference in growth rates or O_2 evolution rates versus wild type. For further discussion interested readers should consult the reviews by Burnap and by Chow and Aro, respectively [12,33].

1.3.2. Intracellular Cluster re-assembly—The rate of the Mn_4Ca cluster assembly depends critically on the local concentrations of free Mn^{2+}, Ca^{2+}, bicarbonate and the pH. Recently, estimates have been provided of intracellular concentrations of these ions in a few cyanobacteria. The Mn content of cyanobacterial cells is generally well in excess of that needed to supply all PS II complexes. However intracellular distribution and transport are not as well known. The capsular peptidoglycan comprising the cyanobacterial envelope (cell wall) plays a major role in concentrating free Mn^{2+} from extracellular solution [40]. Mature cells of *Synechocystis* sp. PCC 6803 take up or exchange free Mn^{2+} at a rate of about 2×10^6 Mn^{2+}/cell in a period of 30 minutes [41]. There are two pools of intracellular Mn^{2+} that have been identified [42]. The largest pool, known as pool A, comprises ~10^8 atoms/cell, is found closely associated with the outer membrane possibly on either the outside or the inner leaflet (periplasm). This pool can be removed by EDTA, is electrogenically generated under light and can be prevented by electron transport inhibitors (DCMU) or abolished by proton uncouplers (like CCCP) that collapse the proton-motive force across the membranes. It thus can be inferred that uptake is energetically coupled to ATP hydrolysis. A tightly associated second pool B comprises ~1.5×10^6 atoms/cell, is not affected by EDTA, light or proton uncouplers and is found in the inner membrane (cytoplasm). Under Mn^{2+} starvation conditions, pool B contains about 10^5 Mn/cell which is essential for photosynthesis, of which the majority is targeted to PSII. By comparison, the marine cyanobacterium *Synechococcus* sp. PCC7002 contains 1.5×10^6 Mn/cell in pool B, while the non-oxygenic purple bacterium *Rhodobacter capsulatus* contains 1% of this amount. Also, two-component regulatory machinery for the sensing of

extracellular Mn^{2+} concentrations and maintenance of intracellular Mn homeostasis in cyanobacteria and non-photosynthetic prokaryotes has been found recently [43].

Intracellular transport of transition metal ions used in enzymatic machinery is typically under tight control by proteins or small molecule chelators that ensure proper targeting of the metal to its final destination and also protect the nascent system from unwanted reactions. These 'chaperone' proteins are widely distributed in the case of iron and copper regulatory systems. The thermodynamic potentials for aqueous Fe^{2+}/Fe^{3+} and Cu^{+}/Cu^{2+} metals indicate that these metals are susceptible to redox changes within cells and thus will undergo major changes in speciation if not coordinated during transport. Thus, it may seem curious that no essential chaperone protein has yet been identified for delivery of Mn^{2+} to the apo-WOC-PS II complex during biogenesis. The explanation is likely due to the inaccessibility of the Mn^{3+} oxidation state in aqueous media at neutral pH owing to the large thermodynamic barrier which prevents Mn^{2+} oxidation (standard reduction potential for Mn^{3+} 1.2 V at pH 7 vs NHE). Moreover, divalent Mn^{2+} with its spherical electronic distribution and half-filled $3d^5$ electronic configuration forms relatively weak coordination complexes with all monodentate O, N, and S ligands [44]. Thus, free Mn^{2+} does not generally associate tightly with the internal machinery of the cell unless there are pre-organized chelation sites present with multiple ligand donors. Generally, the latter sites are specific for ions of a particular size, charge and dehydration energy so that biosynthetic discrimination is almost always ensured. A remarkable example of these rules is illustrated later in the example of the competition between Mn^{2+} and Cs^{+}. Surface electrostatics also play a major role in guiding metal ions to their functional binding sites and this mechanism is important for steering Mn^{2+} to the apo-WOC-PS II site[45]. Binding of aquo-Mn^{2+} to the high affinity site in apo-WOC-PS II has been shown to be influenced by three factors: pH, bicarbonate ions and Ca^{2+}, which are each discussed in the following sections. Although no known chaperones for Mn^{2+} insertion appear to exist as discussed above, repair of the PS II protein complex caused by light absorption does involve chaperone-like proteins [46,47].

2.1 Apo-WOC-PSII preparation and instrumentation for sensitive O_2 detection

In order to carry out *in vitro* studies of the photodamage and photorepair processes, numerous approaches have been reported to extract the Mn_4Ca cluster from the native PSII. Here, we briefly summarize our most recently improved approach as compared to previous methods which have been found to either damage the protein as they cause low photoactivation yields, or cannot fully remove all Mn^{2+} bound to the protein complex. For a representative schematic of the process see Fig 2. An early reported method using TRIS buffer has been used extensively in this field, but has been found to be incapable of achieving even moderate photoactivation yield (supposedly, because of denaturation of the protein and also the generation of *in situ* TRIS radicals)[48] Also, hydroxylamine has been used to reduce the Mn ions and thus make the Mn_4Ca cluster labile. In this method it is argued that only the 17 and 12 kDa proteins are removed similar to TRIS treatment. However, hydroxylamine has been found to be difficult to wash away and thus interferes with the re-assembly process. We and others have developed milder methods for removal of the inorganic cofactors and extrinsic proteins from PS II complexes (apo-WOC-PS II) which is essential for quantitative work leading to high photoactivation yields and reproducible kinetics [45,49,50]. The preferred method relies on short duration incubation of PSII particles at high pH and washing with excess Mg^{2+} to remove both manganese and calcium. When excess Mg^{2+} is used, it results in removal of all three extrinsic proteins. SDS gel chromatography has shown quantitative loss of the extrinsic polypeptides psbQ, psbO and psbP from spinach PSII [51].

Our own studies of photoactivation were performed using a modified Clark-type electrochemical cell for the detection of dissolved O_2 gas in photosynthetic samples[45,52]. It

enabled measurements of O_2 concentration with exceptional sensitivity (50 femtomoles O_2), micro-volume sample (5 μL), and 10-fold higher time-resolution than the commercially available Clark electrodes. The electronic layout and novel material used have been described and circuit diagrams are available upon request. Using this photoactivation instrument has enabled kinetic resolution of the first two steps prior to the rate-limiting step in the assembly of the inorganic cofactors [45,52]. The steps that follow the rate-limiting step are not individually resolved, but their Mn stoichiometry needed to restore O_2 evolution has been accurately determined. Photoactivation follows a two-step sequence, as originally postulated by Cheniae and Tamura on the basis of steady-state O_2 yield measurements[53] and confirmed by Miller and Brudvig [54]. The O_2 recovery kinetics is fitted to a two exponent fitting function that is a general solution to the model in Scheme 1 with rate constants k_1, k_{-1} and k_2. Kinetic resolution of these steps has revealed a reversible, light-dependent lag phase where no O_2 is produced, followed by a single exponential recovery phase [55]. The kinetic resolution provides values of the three rate constants (k_1, k_{-1} and k_2). The sensitivity of the cell has permitted measurement of these rate parameters using sub-stoichiometric (up to hundreds of fold higher concentrations) of Mn^{2+}/PSII.

2.2 Metal ion cofactor

2.2.1 Manganese—Mn appears to be unique in catalyzing O_2 evolution in all oxygenic phototrophs. No other metal ions have been found to date that can replace it. We have examined several metal ions as potential surrogates for Mn^{2+} in the assembly process of spinach apo-WOC-PSII [11]. These studies were conducted by replacing Mn^{2+}, while keeping all other components fixed at the optimal concentrations for Mn-dependent photoactivation (Cl^-, Ca^{2+} and the electron acceptor ferricyanide). The following metal ions were found to inhibit Mn-dependent photoactivation with varying affinities and none were found capable of supporting O_2 evolution in the absence of Mn^{2+} (Cs^+, Ba^{2+}, VO^{2+}, V^{3+}, Cr^{3+}, Fe^{2+}, Co^{3+}, Ni^{2+}, Cu^{2+}, Zn^{2+}, MoO_4^{2-}, Ru3+, Rh3+, Re3+, UO_2^{2+}). However, only a very limited range of conditions were studied: fixed pH 6 (optimal photoactivation yield using native cofactors) and concentrations of Ca^{2+}, Cl^- and electron acceptor. Other pH and concentration conditions ought to be examined before it is known for sure whether Mn can be replaced. The photoactivation process has been studied over a 250-fold range of Mn^{2+} concentrations and it was found that a Mn^{2+}/Ca^{2+} ratio about 1:500 achieves optimal photoactivation yield, extending over the physiological range of concentrations[49]. At higher ratios an aberrant pathway is followed that photooxidizes too much Mn^{2+}, while at lower ratio insufficient Mn^{2+} results in photodamage.

To date, manganese has been found invariably in all PSII-WOCs *in vivo* and is a required cofactor for photoactivation *in vitro*. Several factors may have conspired to make manganese the universal metal for catalyzing water splitting in all oxygenic phototrophs. Open shell transition metals are the clear winners versus main group atoms at storing/delivering large units of energy in the form of redox reactions, e.g., atom transfer reactions, in contrast to acid-base or electrostatic-induced chemistry (eg., Mg^{2+}, Ca^{2+}, Zn^{2+}, Cl^-, etc.) and ion concentration gradients (Na^+, K^+, H^+). This preference arises because transition metals store and deliver energy in the form of both charge (the number of electrons) and bond strengths (potential and kinetic energy of electrons and nuclei). Their versatility originates from the greater number and smaller energy spacing of their valence d-orbitals which facilitates matching with substrate orbitals for maximal bond strength and accommodates a wider range of geometries[56]. A direct consequence is that the geometrical constraints can be relaxed in cases where the redox changes involve non-bonding d-orbitals. For the same reasons, the activation barriers between redox states in multi-step catalysis are usually lower.

Phototrophs take up Mn^{2+} but use it in the Mn^{3+} and Mn^{4+} oxidation states in the WOC. Mn^{2+} is highly soluble, has weak or modest affinity for simple ligands, speciates as the simple aqua cation in water over a wide pH range and is readily transported into cells by a variety of transport systems. Mn^{2+} is chemically stable in neutral solutions. It auto-oxidizes in O_2-saturated solutions only above pH 9.5 where most phototrophs do not function, or at ambient pH only if exceptionally strong chelaters are accessible to stabilize the resulting Mn^{3+} (e.g., pyrophosphate). Hence, there is usually no need for chaperone proteins in the cell to deliver Mn^{2+} or to protect the cellular matrix from auto-oxidation. Chaperones for manganese have not been identified (yet) for assembly of the WOC during the PSII repair process. This simplification led to a great savings in energy and complexity for the primitive phototroph that first used Mn^{2+} over other more abundant redox metals (Fe^{2+}) in the anaerobic world when oxygenic photosynthesis was invented. The redox potential for oxidizing $Mn^{2+}(aq) \rightarrow Mn^{3+}(aq)$ $E^0 = 1.2$ V closely matches the redox potential of Chl-a containing reaction center (> 1.2 V), unlike the majority of other soluble transition ions. Thus, the emergence of Chl-a containing phototrophs enabled the photooxidation of Mn^{2+} to occur on the surface of Chl-a proteins. The resulting Mn^{3+} binds more tightly by ca. 10^{12}–10^{15} and thus would be longer lived at the protein site. Moreover, loss of the redox energy by charge recombination is greatly slowed owing to the energy released upon dissociation of a proton to form $[Mn^{3+}(OH^-)]^{2+}$ ($pK_a \sim 0$). Energetically downhill direct electron-hole recombination without reprotonation is also greatly slowed owing to the unusually large vibronic distortion that Mn^{3+} produces with its ligand environment (e.g., 1 eV activation barrier for pseudo-rotation of the Jahn-Teller axes in MnF_6^{3-})[56]. Importantly, the photooxidation of the next Mn2+ is catalyzed by formation of the first $[Mn^{3+}(OH^-)]^{2+}$ photoproduct, as the resulting OH^- can serve as a better ligand than water to template the binding of the next Mn^{2+}. The efficiency of this assembly process increases in the presence of bicarbonate which is a surrogate for hydroxide and can exist in neutral pH solutions at concentrations many orders of magnitude higher than hydroxide[13, 57].

2.2.2. Calcium—Ca^{2+} is an essential ion in the photoassembly reaction in all native PSII-WOCs examined to date. If Ca^{2+} is left out of the solution, binding and photooxidation of many more Mn^{2+} occurs (up to 20) to the apo-WOC-PSII protein and no O_2 evolution activity is observable[45,58]. The relative binding affinities of various divalent metals (Mg^{2+}, Ca^{2+}, Mn^{2+}, Sr^{2+}), and the oxo-cation UO_2^{2+} have been characterized [11,59,60]. At low Ca/RC concentrations measurements of the kinetics of photoactivation reveal that the Ca^{2+} binding affinity increases following photooxidation of the first $Mn^{2+} \rightarrow Mn^{3+}$, during which 1 Ca^{2+} binds per PSII [55]. This photooxidation step and Ca^{2+} binding leads to a slow dark process that is uncharacterized but has been postulated to represent a protein conformational change. At high Ca/RC concentrations however, Ca^{2+} is already bound to its effector site and the protein conformation change is induced upon Mn^{2+} photooxidation. This process leads to more rapid uptake and photooxidation of the remaining 3 Mn^{2+} in kinetically unresolved steps [55]. Photoactivation kinetics and EPR spectroscopy reveal that when Ca^{2+} binds in the dark to its specific site it induces the formation of a new intermediate consistent with the bridged species [Mn^{2+}-OH-Ca^{2+}]. Illumination of this species gives rise to loss of a proton, consistent with a [Mn^{3+}-O-Ca^{2+}] intermediate, the existence of which was shown by a freeze-trap experiment and characterized by EPR (see below)[61]. Binding of Ca^{2+} to its effector site, eliminates this pH dependence and locks both g_{eff} and A_Z of the photo-oxidized Mn^{3+} EPR signal at values observed in the absence of Ca^{2+} at alkaline pH. Thus, Ca^{2+} directly controls the coordination environment and binds close to the high-affinity Mn^{3+}, probably sharing a bridging ligand. This Ca^{2+} effect and the pH-induced changes are consistent with ionization of a bridging water molecule, predicting that [Mn^{3+}–(μ-O^{2-})–Ca^{2+}] or [Mn^{3+}–(μ-OH^-)$_2$–Ca^{2+}] are the first light intermediates in the presence of Ca^{2+}. Formation of this intermediate templates the apo-WOC-PSII for the subsequent rapid cooperative binding and photooxidation of 3 additional Mn^{2+}

ions, forming the active water oxidase. The photoactivation and spectroscopic data noted above provide a self-consistent picture locating the Ca effector site as an integral part of the Mn_4 core, in direct association with Mn probably via shared bridging ligands to Mn [28], [61].

Boussac discovered that Sr^{2+} can functionally replace Ca^{2+} in the intact holo-enzyme of PSII membranes and thus, restore O_2 evolution activity [62]. Later it was found that there is a kinetic advantage for uptake of Sr^{2+} versus Ca^{2+} at the Ca-effector site during assembly of the apo-WOC enzyme and it was determined how each of the three rate constants measured by photoactivation are affected [11]. Sr^{2+} was shown to be five times more effective than Ca^{2+} in accelerating the rate of the first two assembly steps (k_1 and k_2) and two times better in retarding the deactivation step (k_{-1}). Sr2+ competes with Ca^{2+} and thus occupies the Ca-effector site of the photoassembled PSII. A 65% lower O_2 evolution yield per flash is obtained for the Sr-photoactivated enzyme, which is very close to the decreased steady-state O_2 evolution rate in the Sr-exchanged holo-enzyme. This decrease in O_2 flash yield is known to reflect a retardation of the rate of the final step, $S_3 \rightarrow S_0 + O_2$ [63]. Thus, the data taken together indicate that Ca^{2+} is clearly involved in accelerating the final step in the S-state catalytic cycle, involving the O-O bond formation reaction. No other metal ion other than Sr^{2+} has been found to functionally replace Ca^{2+} in water splitting. On this basis, it has been proposed that the non-directional bonding properties of these alkaline Earth ions and the ionic charge density of Ca^{2+} are critical for allowing formation of a peroxide intermediate, $Ca^{2+}(O_2^{2-})$, between oxo bridges in the step leading to O_2 evolution from the S_4 state of the Mn_4O_4Ca cluster[25,28]. A role for Ca^{2+} as Lewis acid catalyst for proton ionization of substrate water and generation of a nucleophilic hydroxide has also been considered [24,25], although this ignores the direct effect that Ca^{2+} has on the electronic energy of the Mn ions[28].

2.3 Inorganic Cofactors

2.3.1. Oxide bridges/Proton release—In order to build the Mn_4Ca cluster from its free metal ions it is necessary to deprotonate four or more aqua ligands attached to the initially bound Mn^{2+}. Photoactivation has provided important clues about how this process occurs. Alkaline pH accelerates the rate of Mn-dependent photoactivation by 10-fold between pH 5.5 and 7.5, while the final yield of O_2 per flash follows closely the known pH dependence of the holo-enzyme (peaks at pH 6). The data indicate that protons are released during the first two steps of assembly [11,45]. Direct measurements of proton stoichiometry released during photoactivation have been described using a commercial ISFET (ion-selective field-effect transistor) detector [11]. These measurements reveal that a single proton is released upon photooxidation of the high affinity Mn^{2+} to Mn^{3+} in the presence of Ca^{2+}. The first light-induced assembly intermediate therefore contains one fewer proton than the dark precursor and, if this proton is assumed to originate from ionization of a water ligand, it can be formulated as, $[Mn^{3+}(O^{2-})Ca^{2+}]$ or $[Mn^{3+}(OH^{-})_2Ca^{2+}]$ [61].

2.3.2 Bicarbonate ion—Bicarbonate ion is important not only as a substrate for carbon fixation in the Calvin cycle but also for its role in PSII electron transport efficiency and photoassembly of the WOC cluster in PSII. In recent years the requirement for bicarbonate to observe efficient *in vitro* photoassembly has been shown convincingly [49,50]. In cyanobacteria, either bicarbonate or $NaHCO_3$ is actively taken into the cell via ATP-dependent membrane pumps that control either intake or the expulsion of Na^+. Consequently, bicarbonate uptake is tightly controlled and coupled to the light reactions via photophosphorylation. Three distinct transport systems known as carbon concentration mechanisms (CCM) are involved, including one for CO_2 uptake [64]. The photosynthetic activity of the cyanobacterial CCM is modulated in response to inorganic carbon (C_i), with 50% stimulation at concentrations between a low-affinity, constitutive state (approximately 200 μM) and a high-affinity, induced state (10–15 μ is stored M). C_i intracellularly in the form of HCO_3^- and converted back to

CO_2 in structures called carboxysomes for fixation by the Calvin-Benson-Bassham reactions. This conversion uses enzymes known as carbonic anhydrase which exist in multiple subclasses, including a thylakoid membrane associated carbonic anhydrase[65]. Some alkalophilic cyanobacteria (*Arthrospira* genus) that originate from volcanic soda lakes prefer very high extracellular carbonate concentrations reaching 0.4 to 1.2 M $NaCO_3$. These organisms lack carbonic anhydrases all together[66]} and possess a reversible bicarbonate site within the WOC that is required for O_2 evolution ([67]). This site may be the same as the bicarbonate site associated with the Arg 357 residue of subunit CP43 which when mutated, gives rises to lowered O_2 evolution activity, hypothesized as due to a more energetic two-electron oxidation pathway that forms H_2O_2 [68].

PS II appears to possess its own biochemical machinery for regulating the bicarbonate concentration within the lumenal space near the WOC. A low level of carbonic anhydrase (CA) activity, more than 10^3 slower than typical Zn^{2+}-CA, has been found to be intrinsic to oxygen-evolving PS II membranes [69,70]. A soluble CA activity was found associated with the 33 kDa extrinsic protein of PS II (*PsbO*) and depends on the concentration of Mn^{2+} and Cl^-. However the latter results are at contradiction with earlier work showing that neither Mn^{2+} nor Ca^{2+} have specific binding sites on the spinach 33-MSP when studied as a free protein [71]. Given the low activity and requirement for Mn^{2+} there appears to be no clear physiological significance for this site of bicarbonate activity in PSII *in vivo* [65,72].

Bicarbonate ions efficiently replace alkaline pH buffers by accelerating the rate of photoactivation, while increasing the yield of reactivated centers. This is contrary to the lower yield observed upon increasing the buffer pH above 6. This can be understood as follows: bicarbonate binds to two sites within apo-WOC complex as depicted in Fig 3 and described next. A high affinity bicarbonate site operates at concentrations as low as 10 μM in the presence of stoichiometric Mn^{2+}/PSII concentrations, where it accelerates the first step of Mn^{2+} binding and/or photooxidation [50]. The high affinity bicarbonate site has been attributed to the ionization of protons from carboxylate residues or ion-pairing of cationic residues on the surface of the WOC protein complex. These accelerate the rate of photoactivation by electrostatically attracting Mn^{2+} from solution close to the WOC [49]. The rate stimulation is much like that seen with lipid soluble anions like tetraphenylboron which elevate the water soluble cation concentration at the membrane interface [11]. In more extensive studies covering 10 and 100 fold higher concentrations of Mn^{2+} and Ca^{2+}, respectively, a second, lower affinity, bicarbonate binding site on apo-WOC-PS II has been identified that responds to changes in the concentrations of Mn^{2+}, PSII and bicarbonate. This ternary site produces three-fold larger rate acceleration of photoactivation versus “bicarbonate free” samples containing only residual bicarbonate arising from atmospheric equilibration (6 μM). Recent EPR measurements on the trapped intermediates have shown that bicarbonate serves as an integral native cofactor for the initial steps (as described in detail later in this review). It was speculated that it could furnish an oxo/hydroxo bridge for the formation of the WOC [49]. Since its conjugate acid CO_2 is highly soluble in the membrane phase, there will be higher concentration of bicarbonate near the thylakoid membrane than in bulk solution at equilibrium in any system which gets all of its inorganic carbon from CO_2. At still higher (2-8 mM) concentrations of bicarbonate and Mn^{2+}, the formation of free Mn^{2+}-bicarbonate complexes occurs in solution [73]. The formation of these species coincides with a reduction in the rate of photoactivation (lower reconstitution of O_2 yield). These free $[Mn^{2+}(CO_3)_n]^{(2-n)+}$ complexes appear to serve as competitive electron donors to the reaction center. This competitive electron donation is eliminated if the extrinsic subunits are present in the native PSII-WOC, suggesting that a native role of these subunits is to protect the Mn_4Ca core from external attack by cellular reductants.

The clear involvement of bicarbonate in the photoassembly process has been interpreted in terms of a possible evolutionary role for bicarbonate in promoting selectivity for Mn^{2+} binding

and photooxidation over other divalent metals in the Archean eon when this chemistry was invented. This work is summarized elsewhere [13,74,75].

2.3.3. Chloride ion—The role of chloride ion in photoactivation is not clearly revealed, as its influence occurs only following the rate-limiting step and thus affects only the O_2 evolution activity of the fully assembled cluster [45]. However, it should be stated that it is an essential cofactor, both for the O_2 activity of the native enzyme, and for photoactivation yield, as substitution with nitrate and other surrogate ions inhibits the recovery of O_2 activity of the native enzyme. A chloride binding site directly on the Mn_4 cluster has been inferred by ^{14}N ESEEM studies of competitive azide binding to the chloride site within intact PSII centers [76]. Evidence against a direct ligation to Mn_4Ca cluster has also been put forth by FTIR on chloride depleted nitrate substituted PSII samples[77]. It has been speculated that the role of chloride in the water-splitting mechanism is to participate together with charged amino acid side chains in a proton-relay network, which facilitates proton transfer from the manganese cluster to the medium[78].

2.3.4. Non-native cofactors—Previous studies on photoactivation have also encompassed usage of additional non-native cofactors like tetraphenylboron, histidine and imidazole to accentuate or inhibit the *in vitro* assembly process[11]. Recently borate, $B(OH)_4^-$, a chemical analogue of bicarbonate, has been shown to affect the kinetics of photoassembly of the $CaMn_4O_x$ core at only one of the two aforementioned bicarbonate sites during photoactivation [75]. Borate addition in place of bicarbonate causes a 4 fold stimulation of the rate of photoactivation and a 50% increase in yield of photoassembled PSII centers when using the lowest concentrations of Mn^{2+} ($\leq$ 10 μM Mn^{2+}), at which the high affinity Mn^{2+} site is not occupied. However, unlike bicarbonate ion, when this latter site is occupied at 50–100 fold larger concentrations of Mn^{2+} (and sufficient Ca^{2+}), borate addition shows no effect on the rate of the first Mn^{2+} photooxidation step or the yield of photoassembly. Borate, like bicarbonate, does not affect the second (rate-limiting) dark step of photoactivation which is attributed to a protein conformational change [79]. This indicates that borate acts only at the high affinity bicarbonate site (which is not involved in binding of Mn^{2+}). The borate acceleration of photoactivation seen at the high affinity bicarbonate site is stronger than bicarbonate, which is consistent with its stronger basicity (pK_a = 9.3) vs. bicarbonate (pK_a = 6.3). At this site, borate serves as a base to promote proton ionization or ion-pairing with residues of PSII that are responsible for electrostatic steering of Mn^{2+} to the interface of the unfolded apo-WOC-PSII precursor. In this way, PSII utilizes borate and bicarbonate to elevate the local Mn^{2+} concentration well above the bulk solution concentration. This feature offers a clear advantage for building a multinuclear Mn cluster in which incompletely photoassembled intermediates deactivate by autoreduction unless sufficient Mn^{2+} is available for building the next stable intermediate of the cluster. The absence of a borate effect on the low affinity bicarbonate site indicates selectivity for bicarbonate at the high affinity Mn^{2+} binding site. This is fully consistent with the poor metal coordinating properties of the borate anion compared to bicarbonate anion in solution. The dissociation constant of the borate ion with Mn^{2+} at pH 6.0 is K_D > 0.5 M [75], which is at least 10 fold weaker affinity than bicarbonate [73].

Cadmium ions (Cd^{2+}) are known to inhibit reconstitution of O_2 evolution in spinach PSII in competition with Ca^{2+} [80]. Recently it was shown that Cd^{2+} and Gd^{3+} also inhibit the photoactivation process by binding selectively to the Ca^{2+} effector site, but do not bind to the high affinity Mn^{2+} site [81]. This binding was shown to be competitive and reversible with Ca^{2+}. In the presence of Cd^{2+} a new kinetic pathway of photoactivation occurs in competition with the normal two-step pathway. Paradoxically, this inhibition of O_2 yield is accompanied by a large acceleration of the rate of recovery of O_2 evolution, equal to a 5–10 x faster dark step (k_2, Fig 5) and by a slightly slower deactivation rate of the first light-induced intermediate (reduction of photooxidized Mn^{3+}). The data suggest that the binding of the first Mn^{2+} (e.g.,

the high affinity Mn site) increases by 5–10 fold in the presence of Cd^{2+} bound to the Ca^{2+} effector site, attributable to acceleration of the protein conformational change that limits the overall rate of photoassembly. These data reveal that metal ions that bind to the Ca^{2+} effector site interact with the high affinity Mn^{2+} through mutual positive cooperative binding, yielding greater thermodynamic stability and more efficient binding/photooxidation of the high affinity Mn^{2+}.

2.4 Role of protein subunits in assembly

As noted above, the D1, D2, CP47, CP43 and cytochrome *b*559 subunits comprise the minimal oxygen-producing core of native PS II (a number of small subunits that lack cofactors are also generally present in cores)[22]. A stable CP47RC subcore complex assembles within the thylakoid membrane of cyanobacteria in the deletion mutant lacking the *psbC* gene for CP43 [82]. These complexes can be isolated and are active in electron transport but inactive in O_2 evolution, presumably due to an incomplete Mn cluster. A stable CP47RC subcore complex has been prepared from spinach by removal of CP43 with detergents. Although the CP47RC subcore is devoid of Mn and inactive in O_2 evolution, it is capable of substantial activity (20% vs native control) after reconstitution of the Mn cluster by photoactivation in the presence of the free inorganic cofactors [23]. The aforementioned high sensitivity O_2 electrode/photoactivation cell was absolutely essential for observing this reconstitution. The successful reconstitution of the CP47RC subcore together with the subunit positioning data and XRD of the Mn binding site suggest that a RC subcore lacking CP47, might also be capable of O_2 evolution. However, to date no stable subcore complex lacking CP47 has been isolated to test this hypothesis. The implication is that both CP43 and CP47 play an essential role in creating the conditions needed for efficient photoassembly of a stable Mn_4Ca cluster.

The peripheral protein subunits including the manganese stabilizing protein (MSP) have been shown to play an important role in the rate and quantum yield of photoactivation *in vivo*. Burnap and coworkers have identified that in *Synechocystis* sp. PCC 6803 MSP deletion or mutant altering the binding affinity of MSP responds with higher photoactivation quantum efficiency in whole cells. They argue that absence of MSP [83,84] or, in this case, the altered binding of MSP renders the active site (Mn^{2+} high affinity site) more accessible to incoming Mn^{2+}. Increased accessibility of the active site of H_2O oxidation is shown by a variety of studies showing that the extrinsic PSII polypeptides shield the Mn_4Ca catalyst from attack by exogenous reductants, and the carboxyl ligands to the Mn_4Ca from chemical modification. The increased accessibility of the active site was hypothesized to result in a higher probability usage of the oxidizing equivalents generated by the reaction center for the photooxidation and ligation of Mn atoms rather than becoming dissipated via charge recombination. Another reason for increased quantum yield that they provide was that MSP binding affects protonation/deprotonation of the critical protons necessary for photoassembly. Hence, the absence of MSP may permit more facile deprotonation of the critical ionizable groups and/or shift their pK_a of the ionized/un-ionized equilibrium toward the deprotonated state [85].

Mechanism of Photoactivation

3.1 Two-quantum model and extended models

Through the pioneering work of Cheniae and his coworkers, it was shown that photoactivation is a multi-quantum process and the basic kinetic scheme derived from these original studies remains intact[12], although the molecular details have been significantly extended. Photoactivation involves the formation of two unstable intermediates separated by a dark rearrangement step. The basic features of this model were developed by studying the yield of photoactivation in Mn-depleted samples as a function of both light intensity and flash interval in a train of single-turnover flashes. Cheniae's observation was that the quantum yield for

producing O_2-evolving centers was low at very low light intensities, reached a maximum at intermediate intensities, and was again low at high light intensities. In all cases, the quantum yield of photoactivation was observed to be much lower than the quantum yield of photosynthetic oxygen evolution. They reasoned that photoactivation required at least two quanta of light per reaction center with one of the steps occurring with very low quantum yield. When photon fluxes were low, labile photoproducts decayed before the next quantum of light could advance the photoactivation reaction to the next intermediate. On the other hand, intermediate light intensities suppressed the decay due to photooxidation to the next intermediate in the sequence. The fact that high light intensities also gave low quantum yields led them to postulate that a dark relaxation process occurs after the absorption of the first quantum and must take place before the next quantum can be productively utilized. This interpretation was secured by the outcome of paired flash experiments, which demonstrated that two quanta were sufficient to advance the assembling centers through the low quantum yield phase and required the prediction of both the forward dark rearrangement and the decay process. Experiments from Burnap's lab have used paired flash experiments to reveal a third kinetic phase of photoactivation, presumably representing an alternate pathway to the second intermediate, IM_2[86]. The new rate is 5-10 times faster than the rate-limiting dark rearrangement step that is normally observed. Assuming that the dark rearrangement step is a protein conformational change, Burnap asserts the possibility that a fraction of the centers may already exist in the rearranged state during or shortly after the first light-induced step. These centers are thus able to process the second quantum without the prior delay required by the conformational change.

Since the development of the fast oxygen electrode [52], O_2 evolution measurements have enabled kinetic resolution of these intermediates, as described in a series of publications that have been reviewed [11,13]. Next we review more recent work aimed at trapping these intermediates for spectroscopic characterization.

3.2 Trapping assembly intermediates

Initial attempts to trap the intermediates for spectroscopic characterization have been carried out mainly in three labs (Cheniae, Brudvig, and Dismukes). Apo-WOC-PSII samples prepared by TRIS washing, NH_2OH treatment or chelator treatment all suggested the presence of a dimanganese intermediate that was claimed to be a true kinetic intermediate in overall photoactivation (IM_2) and thus productive in formation of the final Mn_4Ca cluster. However, all these trapping experiments disagreed on one major criterion: the preparation of the initial apo-WOC-PSII sample could not supporting full reconstitution upon photoactivation. Britt and coworkers later showed that photooxidation of Mn^{2+} by apo-WOC-PSII isolated from *Synechocystis* sp. PCC 6803 leads to a trappable Mn^{3+} intermediate characterized by EPR which was assigned to the first light intermediate (IM_1)[87]. Again however, systematic measurements of the fate of this detectable Mn^{3+} intermediate in photoactivation were not reported.

In more recent studies, we have used pulsed-EPR of the Mn^{2+}-apo-WOC-PSII dark intermediate and parallel-mode EPR of the photoconverted Mn^{3+} form to characterize the high affinity Mn intermediate at low temperature. We have used spinach apo-WOC-PSII samples that reconstitute 60% or more of O_2 evolution activity in the photoactivation reaction [49]. The EPR method measured the reversible binding of the photooxidizable Mn^{2+} in the dark—e.g., without interference from light dependent reactions at this site and thus it gives a true measure of the equilibrium dissociation constant for this Mn^{2+} (K_D = 40–50 μM at pH 7.5). This Mn^{2+} site possesses the highest affinity of apo-WOC-PSII and therefore, we associate this photooxidizable site with the previously described "high-affinity Mn^{2+} site" involved in electron donation [88,89] and photoactivation [54,90]. It is noteworthy that all methods that

report a considerably higher affinity (K_D ~ 0.1–3 μM) rely on photooxidation/illumination and thus are not reversible by definition.

3.2.1. Ca^{2+} bound intermediates—We used EPR spectroscopy to characterize the ligand coordination environment of the first photoactivation intermediate (IM_1 and IM_1* in Fig 5), corresponding to a photooxidized Mn^{3+} species bound to apo-WOC-PSII [61]. The interconversion of the intermediates detected by EPR are schematically shown in Fig 4. In the absence of any added Ca^{2+}, this species was shown to exist in two pH-dependent forms differing in terms of strength and symmetry of their ligand fields and whose populations are in equilibrium via a pH-dependent process. Transition from an EPR-invisible low-pH form to an EPR-active high-pH form occurs by deprotonation of an ionizable ligand bound to Mn^{3+}, postulated to be a water molecule: $[Mn^{3+}(OH_2)]\leftrightarrow[Mn^{3+}(OH^-)]$. The EPR-active Mn^{3+} exhibits a strong pH dependence (pH ~ 6.5–9) of its ligand field symmetry deduced from changes to both g_{eff} of the Mn^{3+} EPR signal and independently the ^{55}Mn magnetic hyperfine splitting (ΔA_Z = 22%) and attributed to a protein conformational change. The application of ligand field theory to the change in g_{eff} indicates the rhombicity changes by $\Delta\delta$ = 10%, where δ is the mixing coefficient of the $^5B_{1g}$ ground state (d^4 hole in the $d(x^2\text{-}y^2)$ orbital) with the excited $^5A_{1g}$ state (d^4 hole in the $d(z^2)$ orbital) caused by orthorhombic distortions of a predominantly tetragonal ligand field). The binding of Ca^{2+} at its effector site nearly eliminates this pH-dependence of the Mn^{3+} spectral parameters, with δ becoming constant (4.05 ± 0.05) and A_Z smaller and with greatly reduced variation (4%) in the pH range 6.5 to 9.0. Importantly, both δ and A_Z approximate to those observed at high pH ~ 9 in the absence of Ca^{2+}, and were assigned to ionization of a water ligand, $[Mn^{3+}(OH^-)]$. It was implicated thus that Ca^{2+} binding induces proton ionization from a water ligand in the coordination shell of Mn^{3+} and also organizes the coordination shell to make it more uniform and less susceptible to global protein conformational changes induced by pH. The data are consistent with the formation of an oxide (or di-μ_2-hydroxide) bridge, $[Mn^{3+}(O^{2-})Ca^{2+}]$. Here, Ca^{2+} is proposed to induce ionization of a second water ligand bound to Mn^{3+}, or more plausibly, a second ionization of the bridging hydroxo ligand resulting in a bridging oxide ion. Ionization of the water ligand is coupled to the availability of a local base, B^-, with pK_a~ 6.7 as can be estimated from the pH titration curve. Finally, formation of this intermediate $[Mn^{3+}(O^{2-})Ca^{2+}]$, templates the apo-WOC-PSII for the subsequent rapid cooperative binding and photooxidation of 3 additional Mn^{2+} ions, forming the active water oxidase. However, no experimental evidence characterizing these subsequent intermediates is yet available.

3.2.2. Bicarbonate effect on intermediates IM_1 and IM_1*—Bicarbonate coordination of free Mn^{2+} in water lowers the oxidation potential for photoconversion to Mn^{3+} by a large amount (0.5–0.6 V vs. NHE)[91]. This thermodynamic stabilization is thought to be responsible for the increased stability of the Mn^{3+} photoactivation intermediate that forms in the presence of bicarbonate, as seen by slowing of the recombination reaction that causes its decay[49]. However, evidence for direct interaction between the high affinity Mn^{2+}/Mn^{3+} forms and bicarbonate has been lacking until recently [75]. Two lines of evidence have shown that bicarbonate forms a ternary complex by coordinating directly to Mn^{2+} at the high affinity site in apo-WOC-PSII and increasing the yield of photooxidation to form Mn^{3+}. Parallel-mode CW-EPR spectroscopy has shown that bicarbonate controls the ligand field strength of the high affinity Mn^{3+} ion [92]. In the absence of bicarbonate, g_{eff} decreases monotonously by 0.8% with increasing pH between 6 and 9. This correlation means that the rhombicity of the ligand field of Mn^{3+} decreases with increasing pH. The shallow slope and linearity over 3 pH units suggests a continuous range of protein conformational changes within PSII that gradually transform the local ligand field symmetry at the high-affinity Mn^{3+} site to a more axially symmetric environment as the pH increases. Upon addition of 2–10 mM bicarbonate this pH dependence of g_{eff} disappears and is locked into a more rhombic ligand field environment that

is no longer in equilibrium with the bulk pH. A similar conclusion can be drawn from the pH dependence of the ^{55}Mn hyperfine splitting, A_{ZZ}. In the absence of added bicarbonate, A_{ZZ} decreases monotonically by 16–22 % as pH increases from 6 to 9. Addition of 2–10 mM bicarbonate eliminates this pronounced pH dependence, and locks A_{ZZ} within a narrow range, which is equal to the maximum A_{ZZ} observed at acidic pH in the absence of bicarbonate. Comparison to ligand field calculations and experimental data available for other transition metal complexes indicates that the decrease of A_{ZZ} can be attributed to either expansion of the Mn^{3+} d-orbitals bearing unpaired spins, arising from weakening of electron repulsion with its ligands (lower dipolar hyperfine), or alternatively, to an increase of the ligand-metal covalency at higher pH (lower isotropic hyperfine). To summarize, addition of bicarbonate causes both g_{eff} and A_{ZZ} of Mn^{3+} to confine to a narrow range that is independent of solution pH between 6 and 8. This binding produces a fixed inner coordination environment at the high affinity Mn^{3+} site that is considerably more resistant to environmental pH variations. This effect is specific for bicarbonate as other anions including borate do not affect the Mn site. These data provide compelling evidence that bicarbonate is a native cofactor for the assembly of the Mn_4Ca-core.

The complementary pulsed EPR approach electron spin echo envelop modulation (ESEEM) spectroscopy has been applied to answer whether bicarbonate binds directly to the high affinity Mn^{2+} located in apo-WOC-PSII [75,93]. By comparison of ESEEM data for isotopically labeled ^{13}C- and ^{12}C- bicarbonate, a weak (~1.45 MHz) electron-nuclear hyperfine interaction was clearly resolved at the ^{13}C Larmor frequency. Good simulation of the line-shape and intensity profile was achieved and together with comparison to model transition metal-bicarbonate complexes[73] resulted in the following description of this site: (bi)carbonate is bound as a direct ligand in the first coordination sphere of Mn^{2+} in a bi-dentate mode and thus likely speciating as the carbonate form.

3.2.3 Mechanism of Photoactivation—Fig 5 shows the current molecular mechanism of photoactivation, culminating in formation of the active Mn_4CaO_x core, based on the evidence accumulated from both O_2 recovery kinetics and EPR spectroscopy on the trapped intermediates. Formation of the first Mn^{3+} intermediate involves: 1) diffusion of Mn^{2+} to PSII enhanced by electrostatic attraction from anionic amino acid residues and bound bicarbonate ions; 2) Mn^{2+} binding to the “high affinity” site in the D1 protein likely as [$Mn^{2+}(OH_2)$]. This intermediate is denoted IM_0 and may consist of three dark equilibrated species, including bicarbonate bound, water bound and Ca^{2+} bound forms; 3) A single turnover flash (that starts the assembly process) or photoaccumulation at −20 °C leads to the formation by photooxidation of this bound Mn^{2+} precursor to Mn^{3+} with concomitant loss of a proton (IM_1). This intermediate is unstable until a protein conformational change that occurs in the dark takes place and forms the kinetically more stable intermediate IM_1* [Mn3+-O-Ca2+]; 4) Binding of Ca2+ in the dark to its own specific site occurs either before or after this step, albeit with higher affinity after photooxidation forms Mn^{3+}. This increased affinity reflects cooperative binding energy between Mn^{3+} and Ca2+. Since bicarbonate addition does not affect the k_2 step and also there is no evidence yet for a bicarbonate bound form in this state, the bound bicarbonate from the first photooxidation process may dissociate or be released as CO_2. Ultimately the active site is primed for uptake of another Mn^{2+} which forms a spin-coupled cluster (composition $Mn^{2+}Mn^{3+}Ca^{2+}$) that has not yet been detected by EPR. More detailed spectroscopy has to be carried out in order to trap and characterize the second photooxidation intermediate, IM_2 and those that follow. However, to date no kinetic resolution has been observed in the final photoassembly steps forming IM_2 or later intermediates nor the protein conformational change. Titrations of the four Mn^{2+} ions required for photoassembly has previously shown that they bind irreversibly once the active Mn_4Ca core is assembled[45], implying that the “fast” assembly of the remaining 3 Mn^{2+} reflects favorable interaction energy between Mn ions (cooperative binding). Some evidence has been provided by Dau and

coworkers using EXAFS of another trapped intermediate. They have investigated a thermal disassembly pathway of the native PSII complex which retains a Mn-Mn interaction (~ 2.7 Å separation) in the active site [94]. Activity in photoactivation was not examined in this case.

4. Future Directions

The complexity of the assembly process has inspired two new approaches in order to sort out questions regarding the inorganic chemistry involved. Use of synthetic Mn-complexes as sources of Mn^{2+} for the photoactivation of apo-WOC-PSII is becoming popular. All of the organic ligands that constitute these complexes are more lipophilic and tend to give complexes that have poor solubility in aqueous buffer.

Recently, Klimov and co-workers reported multiple classes of N-donor (bipy-, picolinate- and pyrazine-class) and O-donor (acetates) ligands which can be used to deliver Mn and found that dimeric complexes lead to higher yields of photoactivation [95,96]. Also Liu and coworkers reported 79 % photoactivation yield of apo-WOC-PSII with a Mn^{2+} complex prepared with imidazolyl and phenolic ligands [97]. Although these numbers are impressive, the mechanisms of photoactivation by such complexes have not been studied, so there is no information yet on what sort of intermediate forms during assembly, how many Mn are ultimately bound and the chemical speciation of Mn (Mn^{2+} is a labile ion) in the system. Systematic studies have to carried out on such systems in order to learn ultimately how to assemble complexes on protein scaffolds directly from inorganic complexes.

Another emerging topic is designing artificial photoactivatible systems with specific Mn-binding sites within photosystems that possess an intrinsic chromophore. These permit light induced redox chemistry that drives the binding and photooxidation of Mn^{2+}. This method has not yet been explored fully with artificial peptides. However, Allen and co-workers have demonstrated that a modified bacterial reaction center complex from *Rhodobacter sphaeroides* can be produced that photooxidizes Mn^{2+}, but only in the presence of bicarbonate [74,98]. Their results provide the first evidence that a stable Mn^{3+} binding site can be formed in a bacterial reaction center. This suggests a feasible route for evolution of a primitive precursor to the Mn_4Ca core found universally in contemporary oxygenic reaction centers [13,57]. Construction of biological-inspired completely abiotic synthetic representations of the PSII protein scaffolding and catalytic WOC site are underway in some laboratories[99].

5. Conclusions

This review highlights some of the considerable progress that has been made in understanding the molecular events leading to the biogenesis and repair of the Mn_4Ca-cluster and clarification of the role of the inorganic cofactors including bicarbonate. It also raises several important unanswered questions regarding the kinetic and molecular aspects of the steps in this process. In particular unresolved questions remain that are well suited for future investigation by photoactivation: Why is the quantum yield for photoactivation so low (in plant PSII) and do more efficient photoassemblers exist among other oxygenic phototrophs? Can we engineer organisms for higher quantum efficiency of photoassembly? What is the nature of the protein rearrangement that takes place during the slow dark step? What is the minimal number of single turnover photooxidation steps needed to make an O_2 molecule during photoactivation starting from Mn^{2+}? What types of aborted chemical reactions occur instead of O_2 production in partially assembled clusters or inorganic mutants—eg., does H_2O_2 form? In light of the recent EPR data on early trapped intermediates, it is clear that significant structural insight can be mined that could be applied to characterizing the nature of the final steps of the photoassembly process. This should encourage a more systematic attempt to explore the landscape of alternative metal ions as substitutes for Mn and Ca, consideration of a wider pH range to

overcome chemical speciation limitations of the non-native cofactors, and extension to higher temperatures using thermophiles to overcome activation barriers (< 73 °C is conceivably possible).

Acknowledgements

We thank Drs. A.M. Tyryshkin, D. R. J. Kolling and S. V. Baranov for helpful discussions and careful reading of the manuscript.

ABBREVIATIONS

CCCP
: carbonyl cyanide m-chlorophenylhydrazone

CW
: continuous wave

EPR
: electron paramagnetic resonance

EDTA
: ethylenediaminetetraacetic acid

ESEEM
: electron spin echo envelop modulation spectroscopy

EXAFS
: extended X-ray absorption fine structure

MSP
: manganese stabilizing protein

WOC
: water oxidizing complex

References

1. Holland, HD. Chemical Evolution of the Atmosphere and Oceans. Princeton University Press; Princeton, USA: 1984.
2. Krishtalik LI. Biophysics 1989;34:958–962.
3. Rappaport F, Guergova-Kuras M, Nixon PJ, Diner BA, Lavergne J. Biochemistry 2002;41:8518–8527. [PubMed: 12081503]
4. Renger G. Biochim Biophys Acta 2001;1503:210–228. [PubMed: 11115635]
5. Keren N, Berg A, VanKan PJM, Levanon H, Ohad I. Proc Natl Acad Sci USA 1997;94:1579–1584. [PubMed: 11038602]
6. Zak E, Norling B, Maitra R, Huang F, Andersson B, Pakrasi HB. Proc Natl Acad Sci USA 2001;98:13443–13448. [PubMed: 11687660]
7. Frasch W, Sayre RT. Photosynth Res 2001;70:245–247. [PubMed: 16252169]
8. Gray HB, Winkler JR. Quart Rev Biophys 2003;36:341–372.
9. Alstrum-Acevedo JH, Brennaman MK, Meyer TJ. Inorg Chem 2005;44:6802–6827. [PubMed: 16180838]
10. Lu Y. Inorg Chem 2006;45:9930–9940. [PubMed: 17140190]
11. Ananyev GM, Zaltsman L, Vasko C, Dismukes GC. Biochim Biophys Acta 2001;1503:52–68. [PubMed: 11115624]
12. Burnap RL. Phys Chem Chem Phys 2004;6:4803–4809.

13. Dismukes, GC.; Blankenship, RE. Photosystem II: The Water/Plastoquinone Oxido-Reductase in Photosynthesis. Wydrzynski, T.; Satoh, K., editors. 22. Springer; The Netherlands: 2005. p. 609-626.
14. Hankamer B, Morris E, Nield J, Gerle C, Barber J. J Struct Biol 2001;135:262–269. [PubMed: 11722166]
15. Kashino Y, Lauber WM, Carroll JA, Wang QJ, Whitmarsh J, Satoh K, Pakrasi HB. Biochemistry 2002;41:8004–8012. [PubMed: 12069591]
16. Loll B, Kern J, Saenger W, Zouni A, Biesiadka J. Nature 2005;438:1040–1044. [PubMed: 16355230]
17. Ferreira KN, Iverson TM, Maghlaoui K, Barber J, Iwata S. Science 2004;303:1831–1838. [PubMed: 14764885]
18. Yano J, Kern J, Sauer K, Latimer MJ, Pushkar Y, Biesiadka J, Loll B, Saenger W, Messinger J, Zouni A, Yachandra VK. Science 2006;314:821–825. [PubMed: 17082458]
19. Yano J, Kern J, Irrgang KD, Latimer MJ, Bergmann U, Glatzel P, Pushkar Y, Biesiadka J, Loll B, Sauer K, Messinger J, Zouni A, Yachandra VK. Proc Natl Acad Sci USA 2005;102:12047–12052. [PubMed: 16103362]
20. Nanba O, Satoh K. Proc Natl Acad Sci USA 1987;84:109–112. [PubMed: 16593792]
21. Yruela I, Miota F, Torrado E, Seibert M, Picorel R. Eur J Biochem 2003;270:2268–2273. [PubMed: 12752446]
22. Hankamer B, Barber J, Boekema EJ. Annu Rev Plant Physiol Mol Biol 1997;48:641–671.
23. Buchel C, Barber J, Ananyev G, Eshaghi S, Watt R, Dismukes C. Proc Natl Acad Sci USA 1999;96:14288–14293. [PubMed: 10588698]
24. McEvoy JP, Brudvig GW. Chem Rev 2006;106:4455–4483. [PubMed: 17091926]
25. Dasgupta J, van Willigen RT, Dismukes GC. Phys Chem Chem Phys 2004;6:4793–4802.
26. Siegbahn PEM. Curr Opin Chem Biol 2002;6:227–235. [PubMed: 12039009]
27. McEvoy JP, Brudvig GW. Phys Chem Chem Phys 2004;6:4754–4763.
28. Carrell TG, Tyryshkin A, Dismukes GC. J Biol Inorg Chem 2002;7:2–22. [PubMed: 11862536]
29. Britt RD, Campbell KA, Peloquin JM, Gilchrist ML, Aznar CP, Dicus MM, Robblee J, Messinger J. Biochim Biophys Acta 2004;1655:158–171. [PubMed: 15100028]
30. Yano J, Pushkar Y, Glatzel P, Lewis A, Sauer K, Messinger J, Bergmann U, Yachandra V. J Am Chem Soc 2005;127:14974–14975. [PubMed: 16248606]
31. Debus, RJ. Photosystem II: The Water/Plastoquinone Oxido-Reductase in Photosynthesis. Wydrzynski, T.; Satoh, K., editors. 22. Springer; The Netherlands: 2005. p. 261-284.
32. Hillier W, Wydrzynski T. Biochim Biophys Acta 2001;1503:197–209. [PubMed: 11115634]
33. Chow, WS.; Aro, E-M. Photosystem II: The Light-driven Water:Plastoquinone Oxidoreductase. Wydrzynski, TJ.; Satoh, K., editors. 22. Springer; Dordrecht: 2005. p. 627-648.
34. Keren N, Liberton M, Pakrasi HB. J Biol Chem 2005;280:6548–6553. [PubMed: 15611096]
35. Suorsa M, Regel RE, Paakkarinen V, Battchikova N, Herrmann RG, Aro EM. Eur J Biochem 2004;271:96–107. [PubMed: 14686923]
36. Roose JL, Pakrasi HB. J Biol Chem 2004;279:45417–45422. [PubMed: 15308630]
37. Nixon PJ, Trost JT, Diner BA. Biochemistry 1992;31:10859–10871. [PubMed: 1420199]
38. Lers A, Heifetz PB, Boynton JE, Gillham NW, Osmond CB. J Biol Chem 1992;267:17494–17497. [PubMed: 1517201]
39. Trost JT, Chisholm DA, Jordan DB, Diner BA. J Biol Chem 1997;272:20348–20356. [PubMed: 9252339]
40. Mohamed ZA. Water Res 2001;35:4405–4409. [PubMed: 11763042]
41. Ogawa T, Bao DH, Katoh H, Shibata M, Pakrasi HB, Bhattacharyya-Pakrasi M. J Biol Chem 2002;277:28981–28986. [PubMed: 12039966]
42. Keren N, Kidd MJ, Penner-Hahn JE, Pakrasi HB. Biochemistry 2002;41:15085–15092. [PubMed: 12475258]
43. Bhattacharyya-Pakrasi M, Pakrasi HB, Ogawa T, Aurora R. Biochem Soc Trans 2002;30:768–770. [PubMed: 12196191]
44. Smith, RM.; Martell, AE. Critical Stability Constants. Plenum; New York: 1976.
45. Ananyev GM, Dismukes GC. Biochemistry 1996;35:4102–4109. [PubMed: 8672445]

46. Schroda M. Photosynth Res 2004;82:221–240. [PubMed: 16143837]
47. Schroda M, Kropat J, Oster U, Rudiger W, Vallon O, Wollman FA, Beck CF. Biochem Soc Trans 2001;29:413–418. [PubMed: 11497999]
48. Cheniae G, Martin IF. Plant Physiol 1976;57:25.
49. Baranov S, Tyryshkin A, Katz D, Dismukes G, Ananyev G, Klimov V. Biochemistry 2004;43:2070–2079. [PubMed: 14967047]
50. Baranov SV, Ananyev GM, Klimov VV, Dismukes GC. Biochemistry 2000;39:6060–6065. [PubMed: 10821678]
51. Hunziker D, Abramowicz DA, Damoder R, Dismukes GC. Biochim Biophys Acta 1987;890:6–14.
52. Ananyev GM, Dismukes GC. Biochemistry 1996;35:14608–14617. [PubMed: 8931559]
53. Tamura N, Cheniae GM. Biochim Biophys Acta 1987;890:179–194.
54. Miller AF, Brudvig G. Biochemistry 1989;28:8181–8190. [PubMed: 2557898]
55. Zaltsman L, Ananyev G, Bruntrager E, Dismukes GC. Biochemistry 1997;36:8914–8922. [PubMed: 9220979]
56. Bersuker, IB. Electronic structure and properties of transitioin metal compounds. J. Wiley; New York: 1996.
57. Dismukes GC, Klimov VV, Baranov SV, Kozlov YN, Dasgupta J, Tyryshkin A. Proc Natl Acad Sci U S A 2001;98:2170–2175. [PubMed: 11226211]
58. Chen GX, Blubaugh DJ, Homann PH, Golbeck JH, Cheniae GM. Biochemistry 1995;34:2317–2332. [PubMed: 7857943]
59. Ananyev GM, Murphy A, Abe Y, Dismukes GC. Biochemistry 1999;38:7200–7209. [PubMed: 10353831]
60. Vrettos JS, Stone DA, Brudvig GW. Biochemistry 2001;40:7937–7945. [PubMed: 11425322]
61. Tyryshkin AM, Watt RK, Baranov SV, Dasgupta J, Hendrich MP, Dismukes GC. Biochemistry 2006;45:12876–12889. [PubMed: 17042506]
62. Boussac A, Rutherford AW. Biochemistry 1988;27:3476–3483.
63. Westphal KL, Lydakis-Simantiris N, Cukier RI, Babcock GT. Biochemistry 2000;39:16220–16229. [PubMed: 11123952]
64. Badger MR, Price GD. J Exp Bot 2003;54:609–622. [PubMed: 12554704]
65. Rudenko NN, Ignatova LK, Ivanov BN. Photosyn Res 2007;91:81–89. [PubMed: 17347907]
66. Hillier W, McConnell I, Badger MR, Boussac A, Klimov VV, Dismukes GC, Wydrzynski T. Biochemistry 2006;45:2094–2102. [PubMed: 16475798]
67. Carrieri D, Ananyev GM, Brown T, Dismukes GC. submitted
68. Ananyev G, Nguyen T, Putnam-Evans C, Dismukes GC. Photochem Photobiol Sci 2005;4:991–998. [PubMed: 16307112]
69. Lu YK, Theg SM, Stemler AJ. Plant Cell Physiol 2005;46:1944–1953. [PubMed: 16223737]
70. Lu YK, Stemler AJ. Plant Physiol 2002;128:643–649. [PubMed: 11842167]
71. Hunziker, D.; Abramowicz, DA.; Damoder, R.; Dismukes, GC. Progress in Photosynthesis Research. Biggins, J., editor. I. Martinus-Nijhoff; Dordrecht: 1987. p. 5.597-5.600.
72. Moskvin OV, Shutova TV, Khristin MS, Ignatova LK, Villarejo A, Samuelsson G, Klimov VV, Ivanov BN. Photosynth Res 2004;79:93–100. [PubMed: 16228403]
73. Dasgupta J, Tyryshkin AM, Kozlov YN, Klimov VV, Dismukes GC. J Phys Chem B 2006;110:5099–5111. [PubMed: 16526753]
74. Kalman L, LoBrutto R, Allen JP, Williams JC. Biochemistry 2003;42:11016–11022. [PubMed: 12974637]
75. Dasgupta, J. PhD Thesis. Princeton University; Princeton: 2006.
76. Yu H, Aznar CP, Xu XZ, Britt RD. Biochemistry 2005;44:12022–12029. [PubMed: 16142899]
77. Hasegawa K, Kimura Y, Ono T. Biophys J 2004;86:1042–1050. [PubMed: 14747339]
78. Olesen K, Andréasson LE. Biochemistry 2003;42:2025–35. [PubMed: 12590590]
79. Dasgupta J, Ananyev GM, Dismukes GC. submitted

80. Matysik J, Alia A, Nachtegaal G, van Gorkom H, Hoff A, de Groot H. Biochemistry 2000;39:6751–6755. [PubMed: 10841753]
81. Bartlett JE, Baranov SV, Ananyev GM, Dismukes GC. Phil Trans Roy Soc. In Press
82. Rögner M, Chisholm DA, Diner BA. Biochemistry 1991;30:5387–5395. [PubMed: 1903653]
83. Burnap RL, Qian M, Pierce C. Biochemistry 1996;35:874–882. [PubMed: 8547268]
84. Qian M, AlKhaldi SF, PutnamEvans C, Bricker TM, Burnap RL. Biochemistry 1997;36:15244–15252. [PubMed: 9398252]
85. Qian M, Al-Khaldi SF, Putnam-Evans C, Bricker TM, Burnap RL. Biochemistry 1997;36:15244–15252. [PubMed: 9398252]
86. Hwang HJ, Burnap RL. Biochemistry 2005;44:9766–9774. [PubMed: 16008361]
87. Campbell KA, Force DA, Nixon PJ, Dole F, Diner BA, Britt RD. J Am Chem Soc 2000;122:3754–3761.
88. Debus RJ. Biochim Biophys Acta 1992;1102:269–352. [PubMed: 1390827]
89. Hsu BD, Lee JY, Pan RL. Biochim Biophys Acta 1987;890:89–96.
90. Tamura N, Cheniae GM. FEBS Lett 1986;200:231–236.
91. Kozlov YN, Zharmukhamedov SK, Tikhonov KG, Dasgupta J, Kazakova AA, Dismukes GC, Klimov VV. Phys Chem Chem Phys 2004;6:4905–4911.
92. Dasgupta J, Tyryshkin AM, Baranov SV, Dismukes GC. submitted
93. Dasgupta J, Tyryshkin AM, Dismukes GC. Angew Chem Int Ed. In press
94. Barra M, Haumann M, Loja P, Krivanek R, Grundmeier A, Dau H. Biochemistry 2006;45:14523–14532. [PubMed: 17128991]
95. Li SQ, Chen GY, Han GY, Ling L, Huang DG, Khorobrykh AA, Zharmukhamedov SK, Liu QT, Klimov VV, Kuang TY. J Biol Inorg Chem 2006;11:783–790. [PubMed: 16791637]
96. Han GY, Li J, Chen GY, Ling L, Li SQ, Khorobrykh AA, Zharmukhamedov SK, Klimov VV, Kuang TY. J Photochem Photobiol B 2005;81:114–120. [PubMed: 16154756]
97. Liu B, Shen PP, Shi W, Song YG, Li W, Nie Z, Liu Y. J Biol Inorg Chem 2006;11:626–632. [PubMed: 16791645]
98. Thielges M, Uyeda G, Camara-Artigas A, Kalman L, Williams JC, Allen JP. Biochemistry 2005;44:7389–7394. [PubMed: 15895982]
99. Koder RL, Dutton PL. Dalton Trans 2006:3045–3051. [PubMed: 16786062]

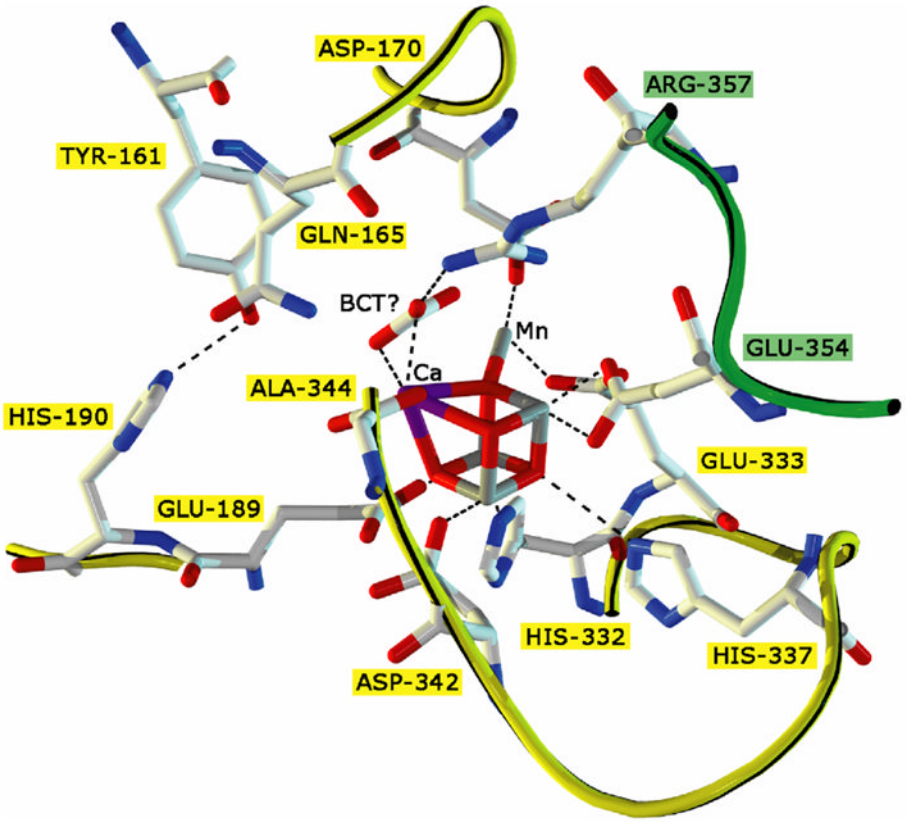

Fig 1.

XRD structural model of the water oxidizing complex (WOC) in Photosystem II adapted from Ferriera et.al.(2004) at 3.5 Å resolution. In the center is the $CaMn_4O_4$-core surrounded by its direct ligands (purple = Ca, grey = Mn, red = O). All amino acids named in a yellow box belong to the D1 subunit, while those in a green box come from subunit CP43. Dashed lines are shown for visual guidance only.

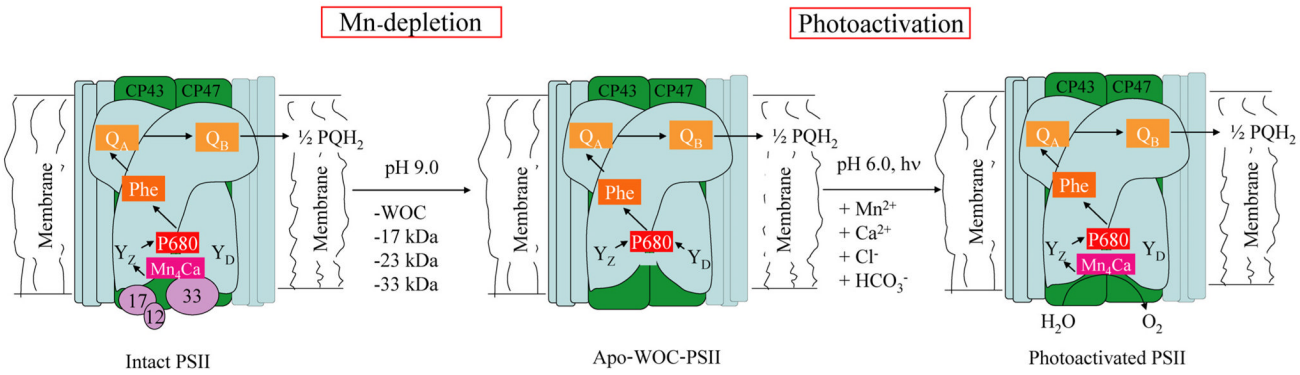

Fig 2.

Scheme summarizing the methodology for removal of Mn_4Ca cluster by high pH treatment, eg., isolation of apo-WOC-PSII particles from isolated spinach PSII membranes, and reconstitution by photoactivation.

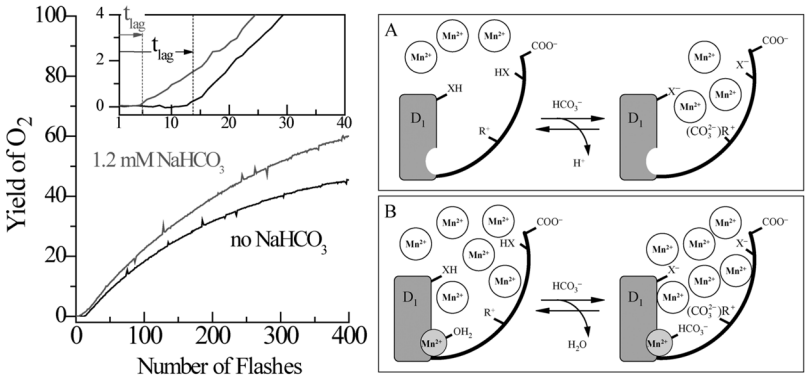

Fig 3.

(Left side) Kinetics of reconstitution of O_2 evolution capacity by photoactivation of the apo-WOC-PSII membranes in the presence of (1) 0 mM, and (2) 1.2 mM, added bicarbonate. Assay conditions are pH 6.0, 1 μM apo-WOC-PSII, 100 μM $MnCl_2$, 100 mM $CaCl_2$, and 1.8 mM $K_3Fe(CN)_6$. The insert expands the first 40 flashes (3 s repetition rate). The vertical dashed lines represent the lag time t_{lag} for each experiment, as derived from fitting the entire kinetics (Baranov et.al. (2004)). (Right side) Two-site model for bicarbonate acceleration of the rate of the first step of photoactivation. (A) The high-affinity bicarbonate site: When the high affinity Mn^{2+} site is unoccupied at low Mn^{2+} concentrations ($[Mn^{2+}] < 30$ μM = K_D [61]), (B) The low affinity bicarbonate site: At high Mn^{2+} concentrations ($[Mn^{2+}] > 30$ μM = K_D), bicarbonate binds directly to the high-affinity Mn^{2+} binding site (Baranov et.al.)(Dasgupta et al., submitted).

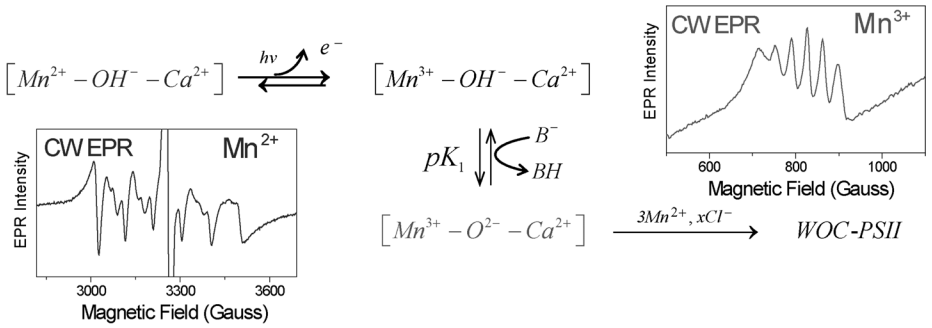

Fig 4.

Schematic representation of the trapped intermediates in the first steps of photoactivation in presence of Ca^{2+}. Protein-derived and non-changing water ligands to Mn^{2+}/Mn^{3+} are not shown. Brackets [ ] represent the high-affinity Mn^{2+} site of apo-WOC-PSII. The CW EPR signals from [Mn^{3+}-O^{2-}- Ca^{2+}] in red and [Mn^{2+}-O^{2-} - Ca^{2+}] in blue is shown. See text for details.

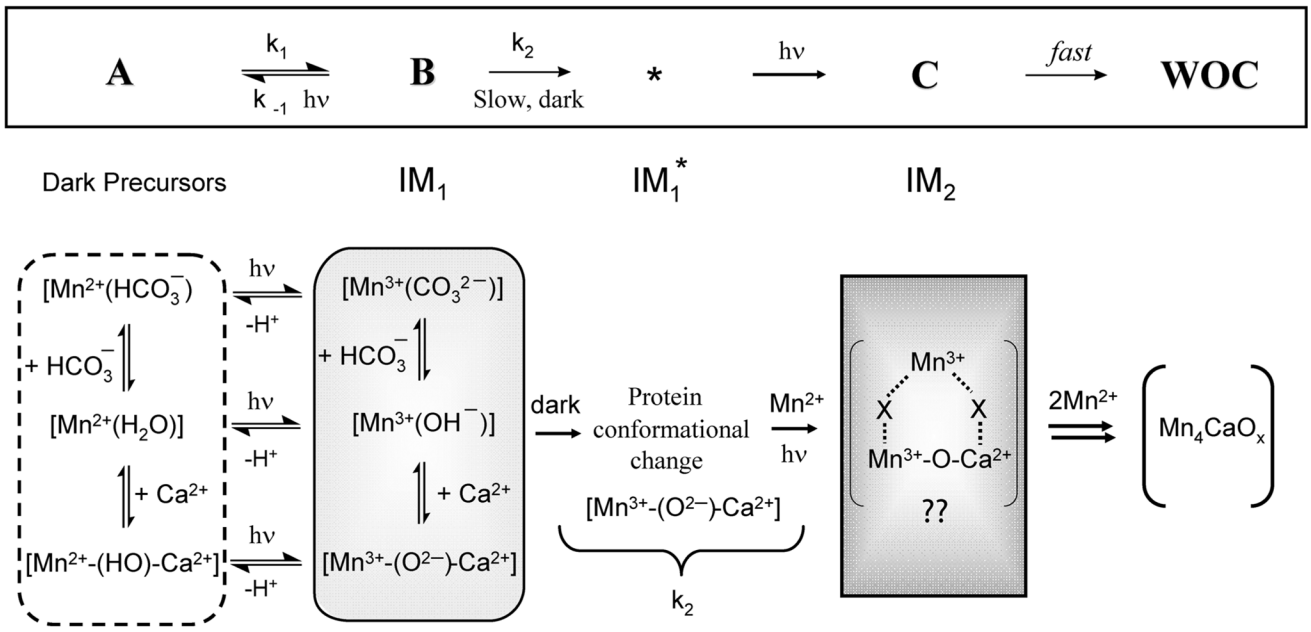

Fig 5.

The sequence of kinetic intermediates (top) formed during assembly of the inorganic core of the WOC by photoactivation (A, B,C). (Bottom) Proposed chemical formulation for intermediates.

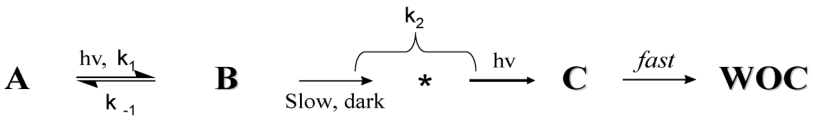

Scheme 1.